

Supplementary Information for

Environmental impact of an acid-forming alum shale waste rock legacy site in Norway

Mila K. Pelkonen^{a,*}, Estela Reinoso-Maset^a, Gareth T.W. Law^b,
Ole Christian Lind^a, Lindis Skipperud^a

^aEnvironmental Chemistry Section, Faculty of Environmental Sciences and Natural Resource Management, Norwegian University of Life Sciences, Aas, Norway

^bRadiochemistry Unit, Department of Chemistry, The University of Helsinki, 00014, Finland

**Corresponding author: mila.pelkonen@nmbu.no*

Environmental Science: Processes & Impacts

August 2024

Section S1. Analytical methodology

S1.1 Ion exchange chromatography

The concentration of anions (F^- , Cl^- , NO_3^- , PO_4^{2-} , SO_4^{2-}) in water samples was determined by anion exchange chromatography using a Lachat IC5000 ion chromatograph (Zellweger Analytix) with a XYZ Autosampler ASX-500 Series and a suppressed conductivity detector. The system was equipped with a Dionex IonPac AG22 guard column (4 x 50 mm), a Dionex IonPac AS22-Fast analytical column (4 x 150 mm), and a Dionex ACRS 500 4 mm suppressor (all from ThermoFisher Scientific). Samples were analyzed in isocratic mode (8.5 run time) with a 4.5 mM Na_2CO_3 / 1.4 mM $NaHCO_3$ eluent at 1.2 mL/min flow rate and a sample loop of 100 μ L. Standard solutions (0.008 – 2 mg/L F^- , 0.08 – 20 mg/L Cl^- , 0.02 – 5 mg/L NO_3^- , 0.004 – 1.0 mg/L PO_4^{2-} , 0.12 – 30 mg/L for SO_4^{2-}) were prepared freshly from 1000 mg/L fluoride, chloride, nitrate, phosphate, and sulfate standards for IC (*TraceCERT*, SigmaAldrich). Reference solutions and certified reference materials (GHL ION Director Multi Reference Solution; Fluka Analytical QC3198 Nutrients – WP whole volume; SigmaAldrich QC3060 Anions – Whole Volume; Environment Canada SANGAMON-03 natural river water) were included at the beginning of the run to check for accuracy and a standard solution and blank were analyzed every 10-12 samples to check for signal and background drift. Method blanks (Milli-Q water, $n = 3$) were used to calculate the limit of detection and quantification (as 3 and 10 times the standard deviation, respectively).

S1.2 Total organic carbon

Total dissolved organic carbon (DOC) in water samples was determined through total inorganic/organic carbon analysis (Shimadzu TOC VCPH/CPN analyzer). Effluent samples were filtered (0.2 μ m) and an aliquot (3-7 mL) was diluted to 10 mL with Milli-Q water (18.2 $M\Omega \cdot cm$). When necessary, solutions were acidified with HCl to $pH < 3$ and stored at $+4^\circ C$ until analysis. Measurements were carried out using high purity air as a carrier to volatilize CO_2 , which was measured by a nondispersive infrared sensor (NDIR). Potassium hydrogen phthalate was used to prepared calibration standard solutions (1 – 25 mg/L C). Methods blanks ($n = 5$) were prepared with MilliQ-water and follow same procedure as the samples. All samples were injected 3-5 times, and the average signal was used for quantification of DOC. The limit of detection and quantification were calculated, respectively, as 3 and 10 times the standard deviation of the method blanks concentrations. The uncertainty of the measurements was 25% for < 1 mg/L and 10% for samples of higher concentration.

S1.3 Gamma spectroscopy

Gamma spectrometry was used to determine the activity concentrations of natural radionuclides of interest in the alum shale samples. Dried and crushed samples in counting geometries were vacuum-packed into aluminum-lined bags to prevent the loss of radon (Rn) gas. The bags were stored for three

weeks prior to analysis to ensure the secular equilibrium between Rn and its progeny. All samples were measured on a Canberra Be5030 HPGe-detector. The collected spectra were analyzed using UniSampo Shaman spectral analysis software and the results were corrected for geometry, density, and elemental composition using the efficiency transfer method (EFFTRAN) developed by Vidmar¹. To maximize the confidence of the results, the activity concentrations were determined using different radionuclides and peaks when possible. The uncertainty of the measurement was calculated as 1 sigma, where the main uncertainty components were efficiency and peak area uncertainties. Uranium-238 was quantified using both Pa-234m and Th-234, assuming equilibrium. Radium-226 activity concentrations were calculated through a weighted average calculation using the progeny nuclides Pb-214 and Bi-214. Uranium-235 activity was calculated from its emission peak at 164 keV and for comparison also from Pa-234m assuming the ratio of 21.4455. Actinium-227 was determined using its progeny nuclides Th-227 and Rn-219. Thorium-232 was determined from Ac-228 and Th-228 from Rn-220 progeny (Pb-212 and Tl-208). Potassium-40 and Pb-210 were quantified from their primary photon emissions.

S1.4 X-ray powder diffraction (XRD)

X-ray diffractograms of ground alum shale were collected at the Swiss Light Source (SLS, Paul Scherrer Institute) on beamline Material Science X04SA operating at ~25 keV.² The operational wavelength ($\lambda = 0.49277 \text{ \AA}$) was accurately determined using a silicon powder standard (NIST SRM 640d). Data was collected in transmission mode in the $0.4^\circ - 150^\circ$ 2θ range with 0.002 as step size using a high-throughput sample handling approach (piezo-driven vibrating sample holders developed by Stenman Mineral Ab) and the MYTHEN III detector with 0.0037° resolution, calibrated with LaB6 crystals and quartz. Diffractograms were converted to Cu-K α radiation wavelength using X'Pert HighScore Plus software. Diffract.Eva V5.1 software was used for peak identification using the Crystallography Open Database (COD Rev212673 2018.12.20) and, based on peak intensity, a semi-quantification (as relative % of identified phases) was obtained. Contributions of < 5% were considered not significant to the overall diffraction pattern.

Table S1. Summary of sample type and parameters measured at the Taraldrud alum shale legacy site during the sampling campaigns comprised in this study between 2020-2023. Sampling was carried out at the reference site (R), precipitation pond (P), mixing zone (MZ), and downstream (DS). A map of the area with the sampling locations can be found in Fig. 1.

<i>Sample type</i>	<i>Sampling locations</i>			
	R	P	MZ	DS
<i>Aquatic environment</i>				
pH	2022	2020, 2021, 2022, 2023	2022	2022
Conductivity	2022	2022	2022	2022
Temperature	2022	2022	2022	2022
ORP	2022	2022	2022	2022
Water samples ^a	2022	2022	2022	2022
Water fractionation ^b	2021	2020	2021	-
<i>Terrestrial environment</i>				
Soil	2021	2021	2021	-
Sediment	-	2021	-	-
Porewater	-	2021	-	-
<i>Plant species</i>				
Grass	2021	2021	2021	-
Fern	2021	2021	2021	-
Wood club-rush	-	2021	-	-
Birch leaves	2021	2021	2021	-
Spruce buds	2021	2021	2021	-
European alder leaves	2021	-	2021	-

^a Unfiltered water samples for anion, total organic carbon, and elemental analysis

^b On-site water fractionation for elemental particle size distribution analysis

Table S2. Characteristics of the alum shale (AS) samples provided by the Norwegian Geotechnical Institute (NGI). The drilling and excavation campaign was carried out at the Taraldrud site in 2021 (sampling locations can be found in Fig. 1). Sample depth, U and Th activity concentrations (in kBq/kg), and acid-forming potential are acquired from the NGI report³, where a detailed description of the samples can be found. Acid-forming potential refers to the rock's buffering capacity, i.e., whether the carbonate content is sufficient to buffer the produced acid or not.

AS sample ID	Sample ID used by NGI	Sampling method	Depth	U (kBq/kg)	Th (kBq/kg)	Acid-forming potential
27	Sjakt 27	Shaft	5-6 m	n.d.	n.d.	n.d.
28	Sjakt 28	Shaft	2-3.6 m	0.67	0.03	no
29	Sjakt 29	Shaft	2-3 m	0.23	0.01	no
31	Borhull 31	Borehole	3.7 m	0.63	0.04	maybe
33	Borhull 33	Borehole	6.6 m	0.71	0.03	yes

n.d. = no data available

Table S3. Certified and standard reference materials (CRM/SRM) used for quality assurance during solid and aqueous phase analysis. The reference materials were run in parallel to the samples throughout the applied method (see main text section 2), and measured concentration values were compared to the certified and reference values, which have an associated 5% uncertainty. The deviation from the true value is reported in % for each element and method's accuracy lower than 80% are highlighted in bold (i.e., difference > 20%).

Element/ Value	CRM/SRM name Concentration Unit	2710a Montana I soil		2711a Montana II soil		NCS DC73325 soil		NCS ZC73007 soil		IAEA-448 oil field soil		IAEA-314 stream sediment		CRM 85113 nutrients in soil	
		Certified value	Difference (%)	Certified value	Difference (%)	Certified value	Difference (%)	Certified value	Difference (%)	Certified value	Difference (%)	Certified value	Difference (%)	Certified value	Difference (%)
Mg	g/kg	7.34	11	10.7	8.4	1.568	16	5.065	5.8	n.d.		n.d.		n.d.	
Al	g/kg	59.5	8.2	67.2	3.0	154.857	3.3	94.47	1.3	n.d.		n.d.		n.d.	
S	g/kg	n.d.		n.d.		0.26	< LOD	0.261	4.2	n.d.		n.d.		n.d.	
Ca	g/kg	9.64	2.6	24.2	1.2	1.143	9.0	2.859	1.7	n.d.		n.d.		n.d.	
Cr	g/kg	23	18	52.3	15	0.41	0.0	0.067	< LOD	n.d.		n.d.		n.d.	
Mn	g/kg	2.14	9.3	0.675	8.7	1.78	3.4	0.441	3.4	n.d.		n.d.		n.d.	
Fe	g/kg	43.2	5.1	28.2	0.35	131.2122	2.1	42.285	10	n.d.		n.d.		n.d.	
Co	mg/kg	5.99	12	9.89	4.3	97	6.2	13.6	3.7	n.d.		n.d.		n.d.	
Ni	mg/kg	8	< LOD	21.7	< LOD	276	7.2	27.4	< LOD	n.d.		n.d.		n.d.	
Zn	g/kg	4.18	3.6	0.414	2.4	0.142	9.1	0.1	2.0	n.d.		n.d.		n.d.	
Cu	g/kg	3.42	5.3	0.14	3.6	0.097	7.2	0.032	0.94	n.d.		n.d.		n.d.	
As	mg/kg	1540	10	107	7.3	4.8	17	18	< LOD	n.d.		n.d.		n.d.	
Mo	mg/kg	n.d.		n.d.		2.9	6.6	1.15	< LOD	n.d.		n.d.		n.d.	
Cd	mg/kg	12.3	8.9	54.1	5.2	0.08	22	0.25	9.6	n.d.		n.d.		n.d.	
Sn	mg/kg	n.d.		n.d.		3.6	7.8	12.4	4.0	n.d.		n.d.		n.d.	
Sb	mg/kg	52.5	8.9	23.8	2.1	0.42	< LOD	1.7	26	n.d.		n.d.		n.d.	
Cs	mg/kg	8.25	1.9	n.d.		2.7	10	13.9	2.2	n.d.		n.d.		n.d.	
Ba	mg/kg	792	0.25	730	0.27	180	1.1	411	0.49	n.d.		n.d.		n.d.	
Pb	mg/kg	5.52	3.6	1.4	1.4	0.014	12	0.061	1.1	n.d.		n.d.		n.d.	
Th	mg/kg	18.8	24	15	19	9.1	9.2	28	2.9	n.d.		17.8	9.5	n.d.	
U	mg/kg	9.11	5.2	3.01	12	2.2	1.8	5.9	8.0	49.2	3.7	56.8	2.5	n.d.	
Ra-226	Bq/kg	n.d.		n.d.		n.d.		n.d.		19050	0.46	732	41	n.d.	
CEC	cmol(+)/kg	n.d.		n.d.		n.d.		n.d.		n.d.		n.d.		31	0.0

n.d. = no data provided in the certificate of analysis

< LOD = measurement below method's limit of detection (LOD)

CEC = cation exchange capacity

Table S4. Solution phase equilibria for uranyl ternary complexes and relevant thorium complexes implemented in the minteq.v4.dat database for geochemical modeling of the precipitation pond water using PHREEQC.

Aqueous chemical equilibria	log K	Ref.*
<i>Ternary uranyl carbonate complexes</i>		
$UO_2^{2+} + Ca^{2+} + 3CO_3^{2-} = CaUO_2(CO_3)_3^{2-}$	27.18	a
$UO_2^{2+} + 2Ca^{2+} + 3HCO_3^- = Ca_2UO_2(CO_3)_3^0(aq) + 3H^+$	-0.29	a
$UO_2^{2+} + Mg^{2+} + 3CO_3^{2-} = MgUO_2(CO_3)_3^{2-}$	26.11	a
<i>Aqueous thorium complexes</i>		
$Th^{4+} + H_2O = Th(OH)^{3+} + H^+$	-2.5	c
$Th^{4+} + 2H_2O = Th(OH)_2^{2+} + 2H^+$	-6.2	c
$Th^{4+} + 3H_2O = Th(OH)_3^+ + 3H^+$	-11.00	b
$Th^{4+} + 4H_2O = Th(OH)_4^0 + 4H^+$	-17.4	c
$Th^{4+} + Cl^- = ThCl^{3+}$	1.7	c
$Th^{4+} + F^- = ThF^{3+}$	8.87	c
$Th^{4+} + 2F^- = ThF_2^{2+}$	15.63	c
$Th^{4+} + 3F^- = ThF_3^+$	20.67	c
$Th^{4+} + 4F^- = ThF^0(aq)$	25.58	c
$Th^{4+} + NO_3^- = Th(NO_3)^{3+}$	1.3	c
$Th^{4+} + 2NO_3^- = Th(NO_3)_2^{2+}$	2.3	c
$Th^{4+} + SO_4^{2-} = Th(SO_4)^{2+}$	6.17	c
$Th^{4+} + 2SO_4^{2-} = Th(SO_4)_2$	9.69	c
$Th^{4+} + 3SO_4^{2-} = Th(SO_4)_3^{2-}$	10.75	c
$Th^{4+} + H_2PO_4^- + H^+ = Th(H_3PO_4)^{4+}$	4.03	c
$Th^{4+} + H_2PO_4^- = Th(H_3PO_4)^{3+}$	5.59	c
$Th^{4+} + CO_3^{2-} + 2H_2O = Th(OH)_2(CO_3)^0 + 2H^+$	2.5	c
$Th^{4+} + CO_3^{2-} + 3H_2O = Th(OH)_3(CO_3)^- + 3H^+$	-3.7	c
$Th^{4+} + CO_3^{2-} + 4H_2O = Th(OH)_4(CO_3)^{2-} + 4H^+$	-15.4	b
$Th^{4+} + 2CO_3^{2-} + 2H_2O = Th(OH)_2(CO_3)_2^{2-} + 2H^+$	8.8	b
$Th^{4+} + 4CO_3^{2-} + H_2O = Th(OH)(CO_3)_4^{5-}$	21.8	b
$Th^{4+} + 5CO_3^{2-} = Th(OH)(CO_3)_5^{6-}$	31	c

*References: (a) Dong et al.⁴; (b) Ervanne et al.⁵; (c) TermoChimie database⁶

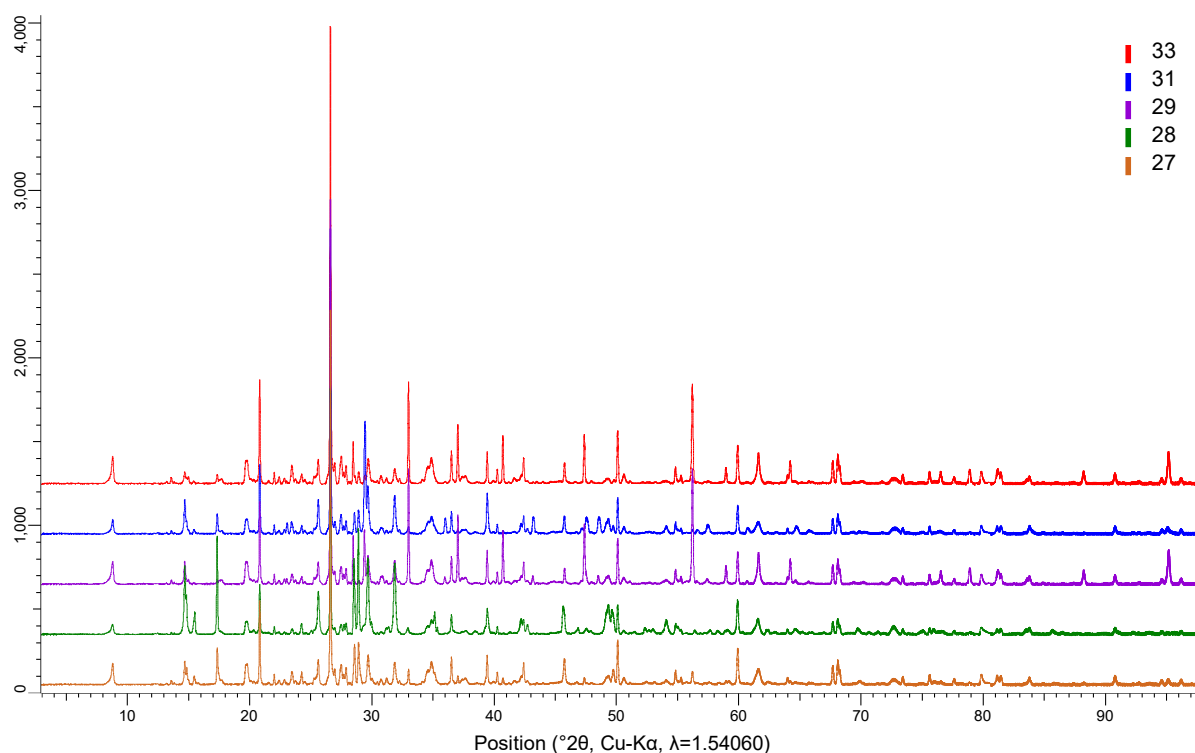


Fig. S1. SR-XRPD diffractograms of alum shale samples of the Taraldrud site (see Fig. 1 for sampling locations).

Table S5. Phase identification and semi-quantification (as % of all phases) obtained from SR-XRPD diffractograms of alum shale samples of the Taraldrud site (see Fig. 1 for sampling locations).

Phase identification			Alum shale sample				
Name	Formula	COD nr.	31	33	27	28	29
<i>Quartz</i>	SiO ₂	9009666	49%	53%	58%	36%	46%
<i>Muscovite</i>	Al _{2.8} Ba _{0.01} Fe _{0.08} H ₂ K _{0.9} Mg _{0.004} Na _{0.07} ° ₁₂ Si _{3.4} Ti _{0.04}	9006326	15%	21%	22%	9%	18%
<i>Orthoclase</i>	AlK _{0.8} Si ₃	1011205		11%	11%	5%	
<i>Jarosite</i>	Fe ₃ H _{6.49} K _{0.51} O ₁₄ S ₂	9010311	5%		9%	22%	
<i>Pyrite</i>	Fe ₂ S	5000115		12%			14%
<i>Pyrite</i>	As _{0.026} FeS _{1.974}	9013070					6%
<i>Bassanite</i>	CaHO _{4.5} S	9005521	14%	3%		28%	10%
<i>Calcium carbonate</i>	CCaO ₃	4502441	16%				6%

Table S6. Activity concentrations (in Bq/kg) and associated measurement uncertainties (in %) of alum shale (AS) samples of the Taraldrud site (see Fig. 1 for sampling locations) obtained by gamma spectrometry. Radionuclides marked with * were considered for isotopic ratio calculations. *Note: K-40 activity concentrations exceed the range for sedimentary rocks (70-900 Bq/kg)⁷ but agree with estimated values based on stable K³, thus it was not discussed further.*

Radionuclide	AS 27		AS 28		AS 29		AS 31		AS 33	
	A _c (Bq/kg)	Unc.	A _c (Bq/kg)	Unc.	A _c (Bq/kg)	Unc.	A _c (Bq/kg)	Unc.	A _c (Bq/kg)	Unc.
U-238* (Pa-234m: 1001.0 keV)	870.0	3.3%	569.0	3.7%	1890.0	3.6%	603.0	5.5%	755.0	5.8%
U-238 (Th-234: 63.3 keV)	796.0	11.4%	580.0	10.6%	1860.0	11.5%	625.0	12.4%	772.0	10.5%
U-235 (163.4 keV)	35.2	4.6%	21.4	4.5%	87.1	4.1%	28.6	8.5%	34.3	11.5%
U-235* (calc. from Pa-234m)	40.6	3.3%	26.6	3.7%	88.3	3.6%	28.1	5.5%	35.2	5.8%
Ra-226 (Pb-214: 295.2, 351.9 keV, Bi-214: 609.3, 1120.3, 1764.5 keV)	1770.0	3.7%	1850.0	3.8%	2030.0	3.9%	1230.0	3.9%	2060.0	3.5%
Th-232 (Ac-228: 911.2, 969.0 keV)	44.0	3.4%	45.7	3.7%	50.1	3.8%	43.1	4.2%	43.1	4.7%
Th-228 (Pb-212: 238.6, 300.1 keV, Tl-208: 583.2, 2614.5 keV)	44.2	3.6%	44.5	3.8%	50.9	3.6%	46.8	3.7%	44.2	4.5%
Ac-227* (Th-227: 234.8, 256.2 keV)	66.6	10.3%	75.4	10.2%	92.1	10.0%	64.2	10.1%	94.8	10.4%
Ac-227 (Rn-219: 401.8 keV)	66.1	8.6%	81.0	8.5%	93.1	9.4%	60.7	9.4%	99.6	9.2%
Pb-210 (46.5 keV)	1900.0	22.9%	1830.0	21.9%	2070.0	23.2%	1180.0	24.4%	2080.0	21.8%
K-40 (1460.8 keV)	1400.0	3.9%	1130.0	4.2%	1090.0	4.7%	1040.0	4.7%	1240.0	5.2%
Isotopic ratios	27		28		29		31		33	
Ra-226/U-238	2.0		3.3		1.1		2.0		2.7	
Pb-210/Ra-226	1.1		1.0		1.0		1.0		1.0	
Ac-227/U-235	1.6		2.8		1.0		2.3		2.7	
Th-228/Th-232	1.0		1.0		1.0		1.1		1.0	

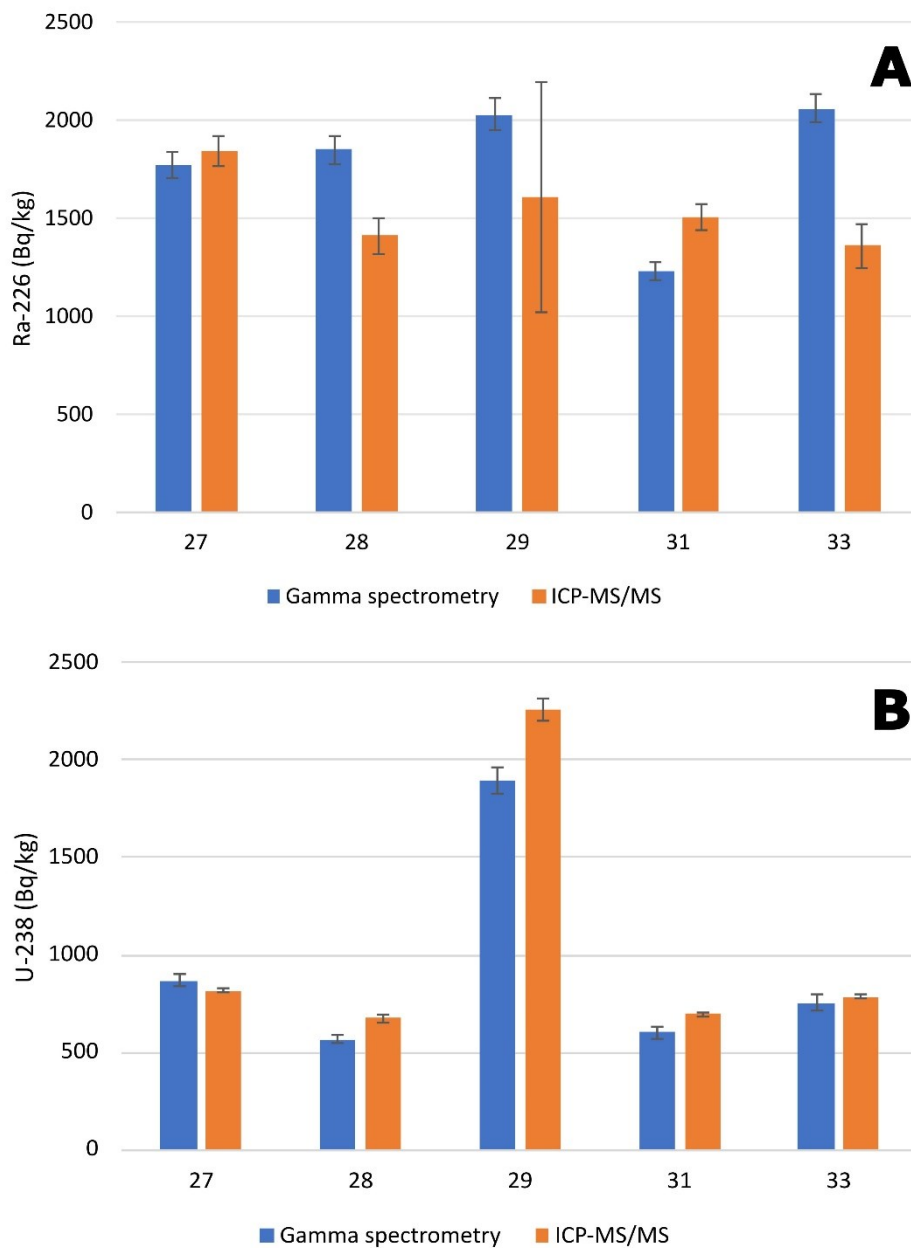


Fig. S2. Comparison of (A) Ra-226 and (B) U-238 activity concentrations in alum shale (AS) samples of the Taraldrud site obtained by gamma spectrometry and by ICP-MS/MS analysis after digestion. Error bars represent the counting uncertainty for gamma spectrometry and the method uncertainty for triplicate samples by ICP-MS/MS analysis. See Fig. 1 for sampling locations.

Table S7. Element concentrations in alum shale (in mg/kg) and leachate (in mg/L) from location 27 of the Taraldrud site (see Fig. 1 for sampling locations). Values were obtained from the NGI report³ to calculate element accumulation from alum shale to leachate and estimate a leachability pattern representative of the source of contamination at the site (i.e., the deposited alum shale waste rock). Accumulation values are normalized with respect to the smaller shale-to-leachate ratio (in this case Ca) to compare leachability behavior.

AS 27			
Element	Alum shale (mg/kg)	Leachate* (mg/L)	Normalized accumulation
Ca	427	584	1.0
Mn	11	7.58	2.0
Na	411	253	2.2
Mg	663	190	4.8
S	27354	1702	22
Fe	3700	196	26
Ni	137	4.92	38
U	61	2.2	38
Cd	3	0.0882	47
Zn	104	2.82	50
Co	29	0.756	52
Cu	193	3.13	84
Al	7198	76.3	129
Th	12	0.052	316
Cr	58	0.0893	888
As	75	0.107	959
Mo	177	0.0642	3771
V	632	0.0725	11922
Pb	82	0.00531	21121
Ba	2900	0.0807	49148

* Leachate pH = 2.9³

Table S8. Concentration limits for elements in fresh waters from current environmental quality standards used in Norway (NO), European Union (EU), and Canada (CA), and the ratio with respect to the quality standards for concentrations measured at the reference site (R), precipitation pond (P), mixing zone (MZ), and downstream (DS) of the Taraldrud site (sampling locations in Fig.1, concentrations in Table 1). Ratios marked in bold represent elements whose concentration in water exceeds the environmental quality standard and “< LOD” indicates concentrations below the detection limit.

Element	Environmental quality standards*		Concentration ratios			
	Limit (µg/L)	Country	R/limit	P/limit	MZ/limit	DS/limit
Cl-	120000	CA	0.4	1.0	0.7	0.7
F-	120	CA	2	22	2	2
NO ₃ -	13000	CA	0.02	0.01	0.03	0.03
Fe	300	CA	0.6	91.1	1.0	0.6
Cr	3.4	NO	< LOD	6.8	< LOD	< LOD
Mo	73	CA	0.03	0.003	0.03	0.03
Ni	4	NO + EU	0.3	550	3	2
Cu	7.8	NO	< LOD	102	< LOD	< LOD
Zn	11	NO	< LOD	94	< LOD	< LOD
Cd**	0.09	NO + EU	< LOD	311.1	1.0	1.0
Pb	1.2	NO	< LOD	7	< LOD	< LOD
As	0.5	NO	0.6	0.9	0.6	0.5
U	15	CA	0.2	56.2	0.4	0.4

*Norwegian and European Union Environmental Quality Standards (AA-EQS)^{8,9}, and Canadian water quality guidelines for long-term exposure to protect aquatic life¹⁰.

**Cadmium limit is dependent on levels of CaCO₃.

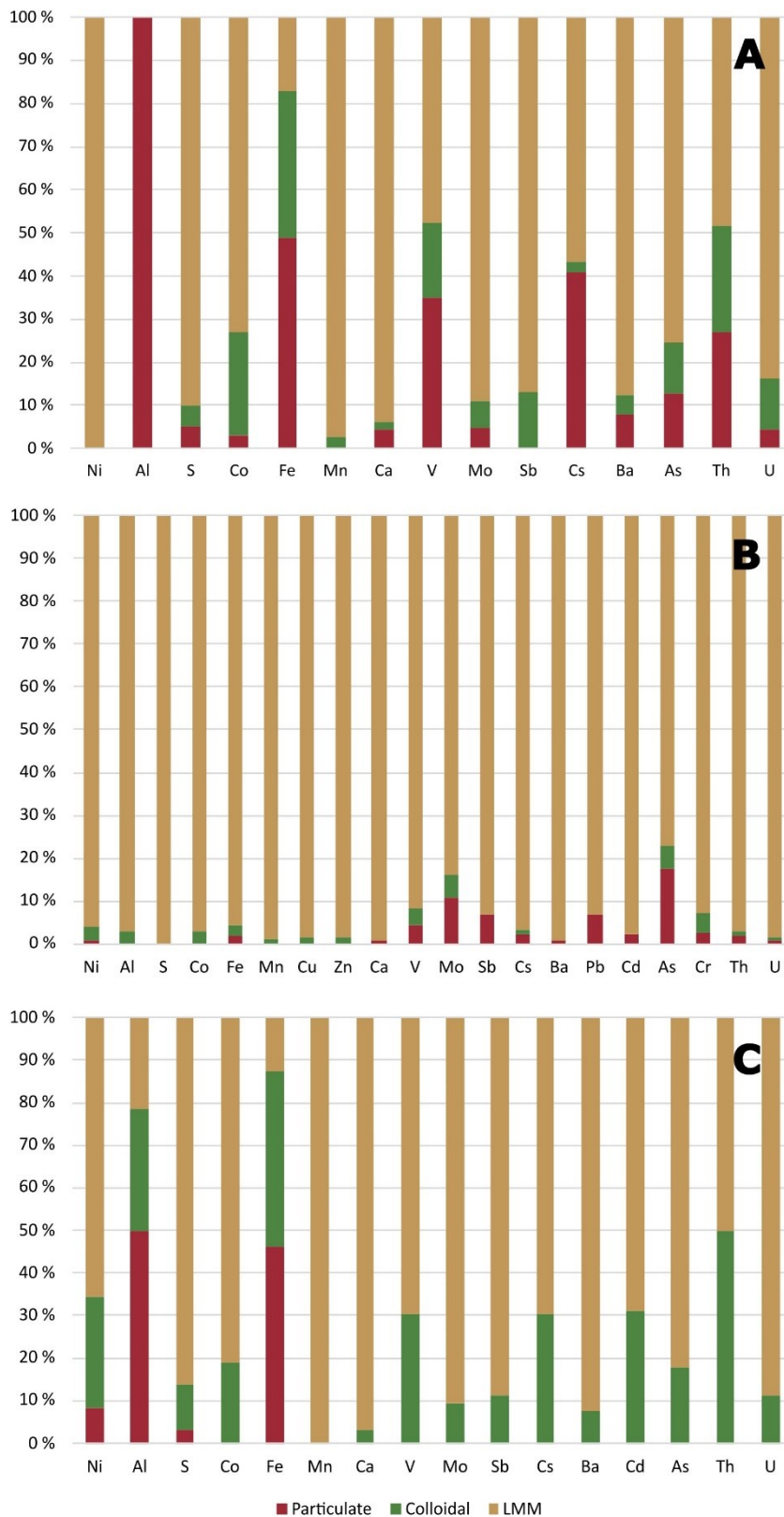


Fig. S3. Elemental distribution with particle size in water samples collected at the: (A) reference site R, (B) precipitation pond P, and (C) mixing zone MZ of the Taraldrud site. Size species were classified as: particulate ($> 0.45 \mu\text{m}$), colloidal ($< 0.45 \mu\text{m}$, $> 10 \text{ kDa}$), and low molecular mass (LMM, $< 10 \text{ kDa}$).

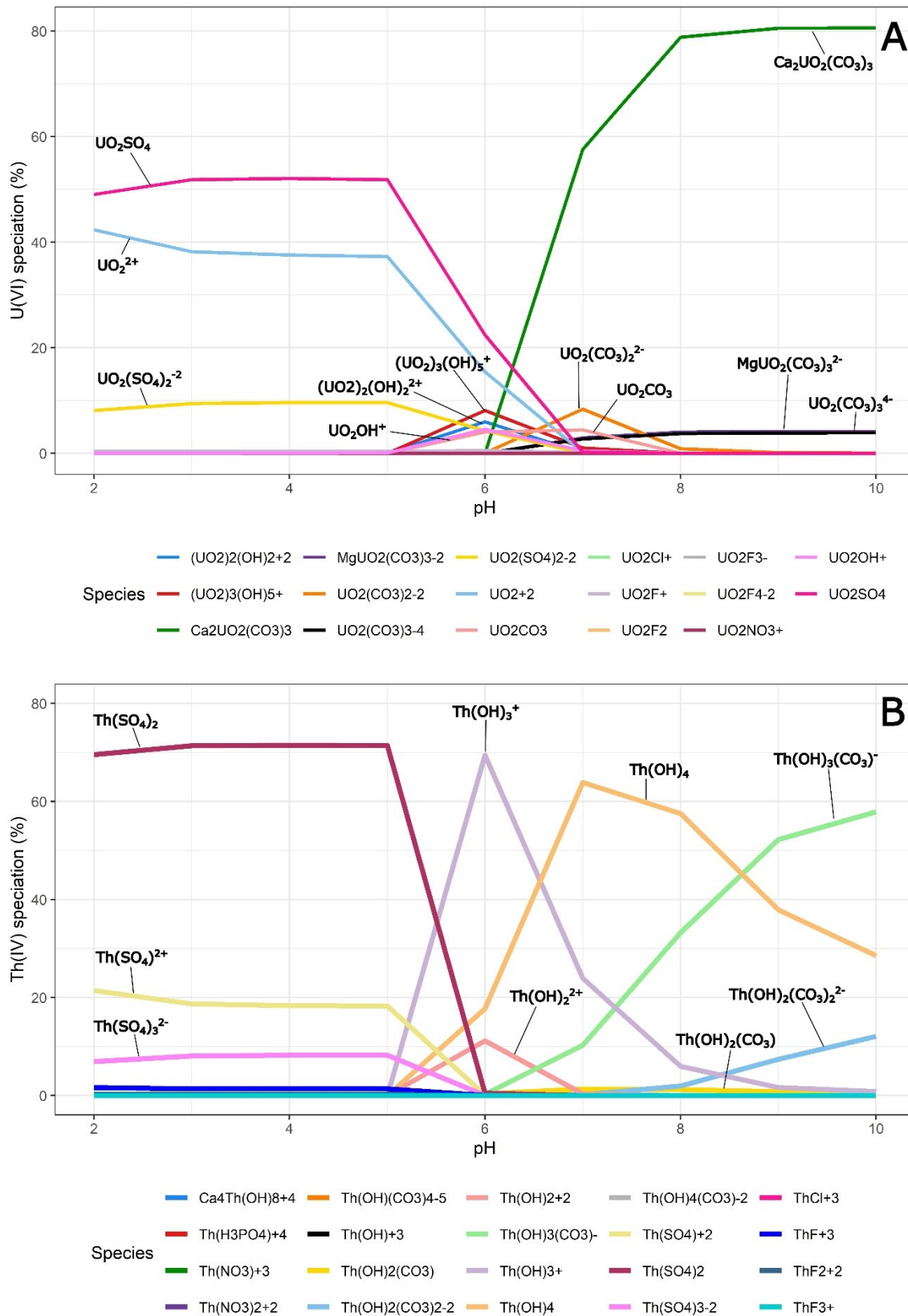


Fig S4. Distribution of aqueous (A) U and (B) Th species in relation to pH under the precipitation pond water conditions (concentrations in Table 1). The speciation was calculated with PHREEQC computer program (see the main text, section 2.5.6 for details).

Table S9. Saturation indices (SI) for mineral phases oversaturated in the precipitation pond water. Thermodynamic modeling was carried out using PHREEQC computer program with minteq.v4 database and experimental data (Table 1). Positive saturation indices (SI > 0) indicate that the solution is oversaturated with respect to a given mineral phase, which imply a higher tendency for the mineral to precipitate at thermodynamic equilibrium.

Mineral phase	Chemical formula	Saturation index (SI)
Anglesite	PbSO ₄	0.30
Barite	BaSO ₄	0.14
Birnessite	MnO ₂	0.10
Nsutite	MnO ₂	0.69
Pyrolusite	MnO ₂	1.16
Cupricferrite	CuFe ₂ O ₄	0.79
Fe(OH) _{2.7} Cl ₃	Fe(OH) _{2.7} Cl ₃	5.10
Ferrihydrite	Fe(OH) ₃	0.10
Goethite	FeOOH	2.88
H-Jarosite	(H ₃ O)Fe ₃ (SO ₄) ₂ (OH) ₆	4.89
Hematite	Fe ₂ O ₃	8.10
Lepidocrocite	FeOOH	2.36
Maghemite	Fe ₂ O ₃	1.08
Strengite	FePO ₄ :2H ₂ O	0.53



Fig S5. Representative pictures of soil core sampling (top) and alum shale waste rocks (bottom) at the Taraldrud site. For soil sampling: a plastic corer tube was vertically inserted into the soil or sediment followed by careful excavation in order to retrieve an intact core. During the sampling at the P and MZ site locations, orange-brown color was observed on the top layers, suggesting the presence of iron-rich solid phases. Alum shale sampling was carried out by NGI in 2021.³

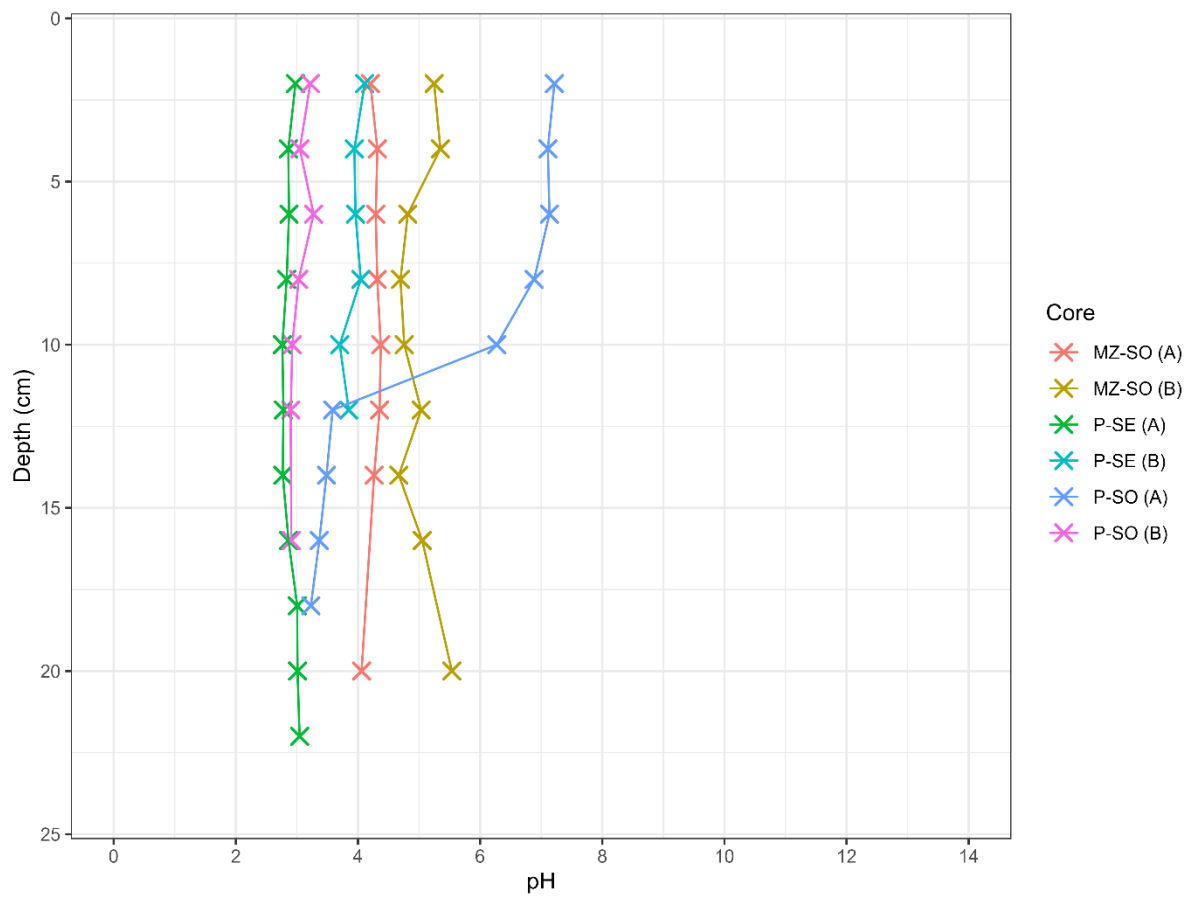


Fig. S6. Depth profile for soil and sediment pH of duplicated cores sampled at the precipitation pond (P) and mixing zone (MZ) of the Taraldrud site (locations in Fig. 1).

Table S10. Summary of significantly different (non-parametric Kruskal-Wallis test, $p < 0.05$) metal concentrations within duplicated soil and sediment cores sampled at the precipitation pond (P) and mixing zone (MZ) of the Taraldrud site (locations in Fig. 1).

Element	Cores		
	P-SO(A)	MZ-SO(A)	P-SE(A)
	P-SO(B)	MZ-SO(B)	P-SE(B)
Mg	x		x
Al	x	x	x
S	x	x	x
Ca	x	x	
V			
Cr		x	
Mn	x	x	x
Fe	x	x	x
Co	x		
Ni		x	x
Cu		x	x
Zn	x	x	
As		x	x
Mo		x	x
Cd	x	x	x
Sn	x		x
Sb			
Cs		x	x
Ba			x
Pb	x	x	
Th	x		x
U		x	x

Table S11. Concentration limits for potentially toxic elements as per Norwegian (NO), Finnish (FIN), and Canadian (CA) quality standards, and the ratios with respect to the recommended limit for measured concentrations in soils from the reference site (R), precipitation pond (P) and mixing zone (MZ) of the Taraldrud site (locations in Fig. 1, concentrations in Table 3). Ratios marked in bold represent elements whose concentration exceeds the environmental quality standard.

Element	Standard values for non-polluted soil*		Concentration ratios		
	Limit (mg/kg)	Country	R/limit	P/limit	MZ/limit
Cu	8	NO	3	13	22
Cr	50	NO	1.7	1.5	1.3
Ni	60	NO	0.7	1.3	1.1
As	8	NO	0.6	1.1	2.3
Cd	1.5	NO	0.1	0.4	0.6
Co	20	FIN	0.8	0.8	0.5
Pb	60	NO	0.0017	0.0007	0.0003
Zn	200	NO	0.6	0.8	0.5
U	500	CA**	0.01	0.10	1.11

*SFT standard values – criteria for non-polluted soil in Norway ¹¹, PIMA guideline values for contaminated soils in Finland ¹², and Canadian soil quality guidelines for residential/parkland for the protection of environmental and human health ¹³.

**Guideline value for soil contact.

Table S12. Concentration thresholds for ecological risks in background sediments used in Norway and the ratios with respect to the recommended limit for measured concentrations in sediment from the precipitation pond (P) of the Taraldrud site (location in Fig. 1, concentrations in Table 3). Ratios marked in bold represent elements whose concentration exceeds the environmental quality standard.

Element	Concentration threshold	Concentration ratio
	Limit (mg/kg)*	P/limit
Cu	20	11
Cr	60	2
Ni	30	2
As	15	0.9
Cd	0.2	2
Pb	25	0.002
Zn	90	1.2

**Concentration thresholds for ecological risks in background sediments from The Norwegian Environment Agency (NEA)¹⁴*

Table S13. Principle component (PC) analysis of the variables measured in soil and sediment cores from the precipitation pond (P) and mixing zone (MZ) of the Taraldrud site (i.e., characterization results of P-SO(A), P-SO(B), MZ-SO(A), MZ-SO(B), P-SE(A), and P-SE(B)). The data was centered and scaled prior to analysis (n = 33). Standard deviation, proportion of variance, cumulative proportion, and eigenvalues are given for PC1-PC4, which all had eigenvalues above 1 and together explained 86.6% of the variance (48.6% PC1, 21.1% PC2, 9.91% PC3, 6.87% PC4). Loading factors above 0.213 are highlighted in bold to show the variables most contributing to each PC.

	PC1	PC2	PC3	PC4
Standard deviation	3.270	2.162	1.477	1.230
Proportion of variance	0.486	0.212	0.099	0.069
Cumulative proportion	0.486	0.698	0.798	0.866
Eigenvalue	10.691	4.674	2.181	1.512
<i>Eigen vectors</i>				
Mg	0.279	-0.152	0.039	0.093
Al	0.259	0.076	0.095	-0.209
S	-0.271	-0.070	-0.153	0.243
Ca	0.162	-0.322	-0.053	0.077
Cr	0.127	0.089	-0.528	0.254
Mn	0.256	-0.225	0.069	-0.005
Fe	-0.277	-0.107	0.055	0.242
Co	0.110	-0.396	-0.121	-0.211
Ni	-0.051	-0.403	-0.207	-0.158
Cu	-0.243	-0.112	-0.206	0.123
Zn	-0.034	-0.425	-0.045	-0.075
As	-0.201	-0.130	0.176	0.176
Mo	-0.258	-0.150	0.202	0.143
Cd	-0.107	-0.316	-0.020	-0.430
Sn	0.250	-0.073	-0.075	0.103
Cs	0.221	0.208	-0.044	-0.370
Ba	0.267	0.017	-0.183	0.211
Pb	0.198	-0.212	-0.201	0.184
Th	-0.124	0.132	-0.506	-0.063
U	-0.245	-0.077	0.146	-0.138
Dry weight (DW)	0.260	-0.030	0.293	0.098
Organic carbon (OrgC)	-0.197	0.150	-0.241	-0.417

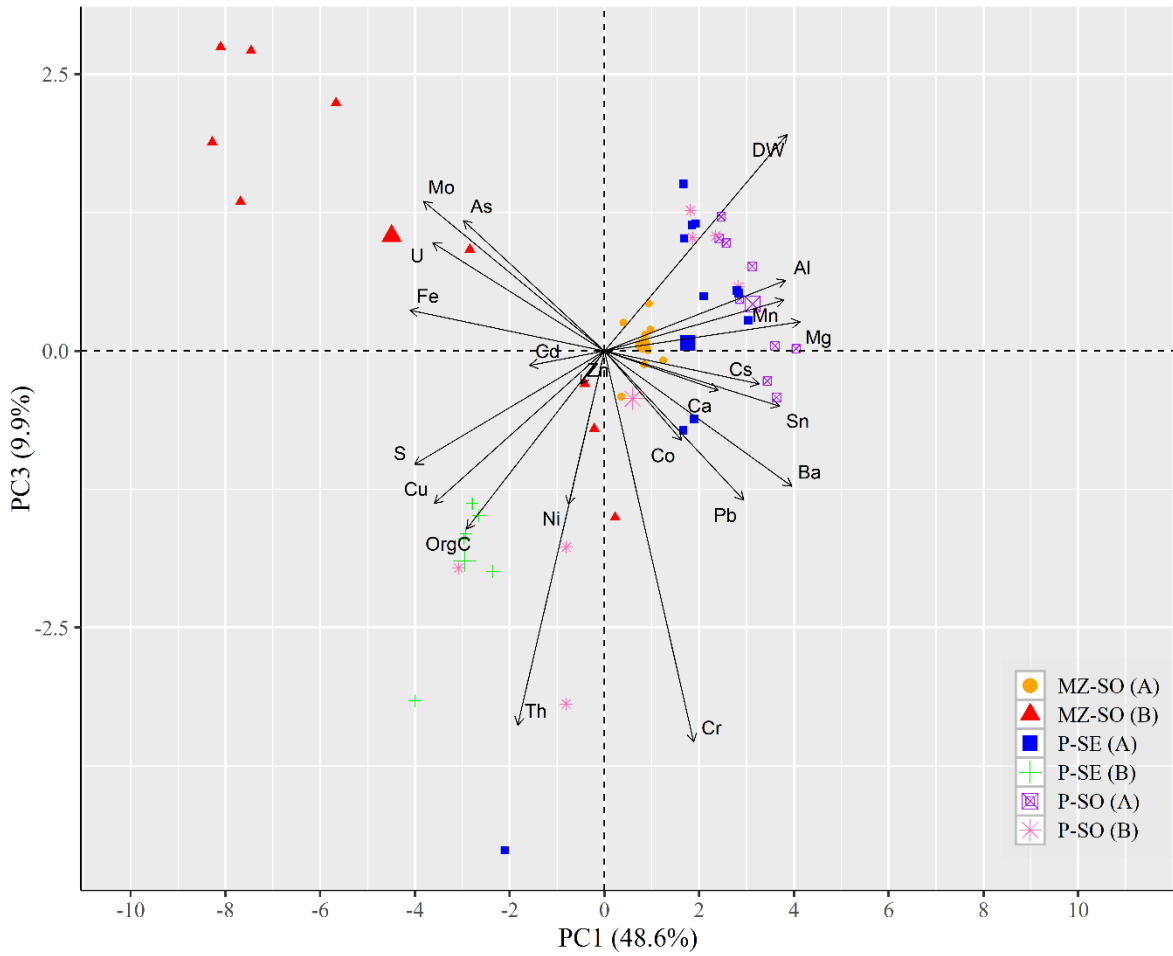


Fig. S7. Principal component (PC) biplot of the characterization results for soils and sediments from the precipitation pond (P) and mixing zone (MZ) of the Taraldrud site. The length of the arrow represents the contribution of the variable to the first and third factor (PC1-PC3) and the size of the sample/location point an individual scoring. Each symbol represents a different sampling dept, different symbols represent different cores. The mean score (barycenter) for each core is presented with a larger symbol.

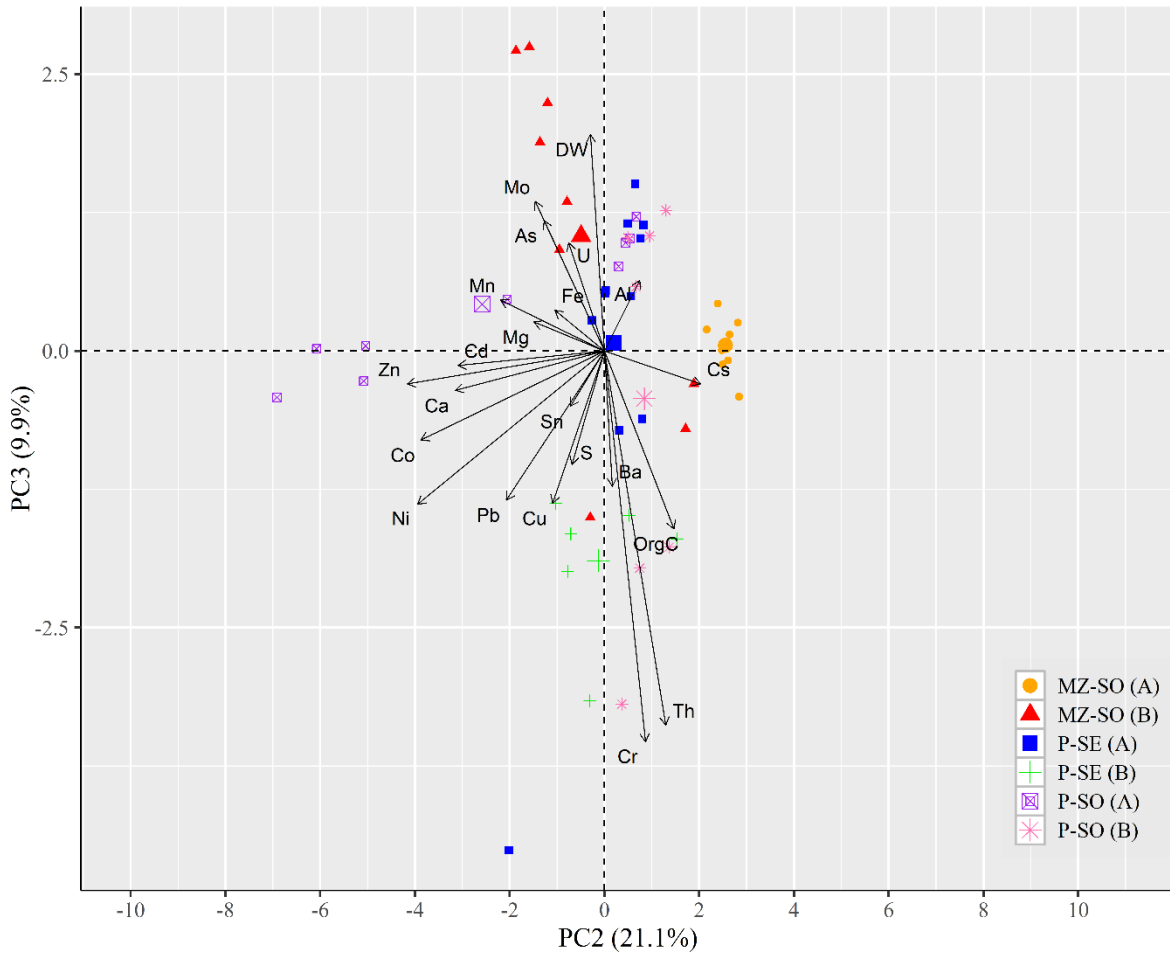


Fig. S8. Principal component (PC) biplot of the characterization results for soils and sediment from the precipitation pond (P) and mixing zone (MZ) of the Taraldrud site. The length of the arrow represents the contribution of the variable to the second and third factor (PC2-PC3) and the size of the sample/location point an individual scoring. Each symbol represents a different sampling dept, different symbols represent different cores. The mean score (barycenter) for each core is presented with a larger symbol.

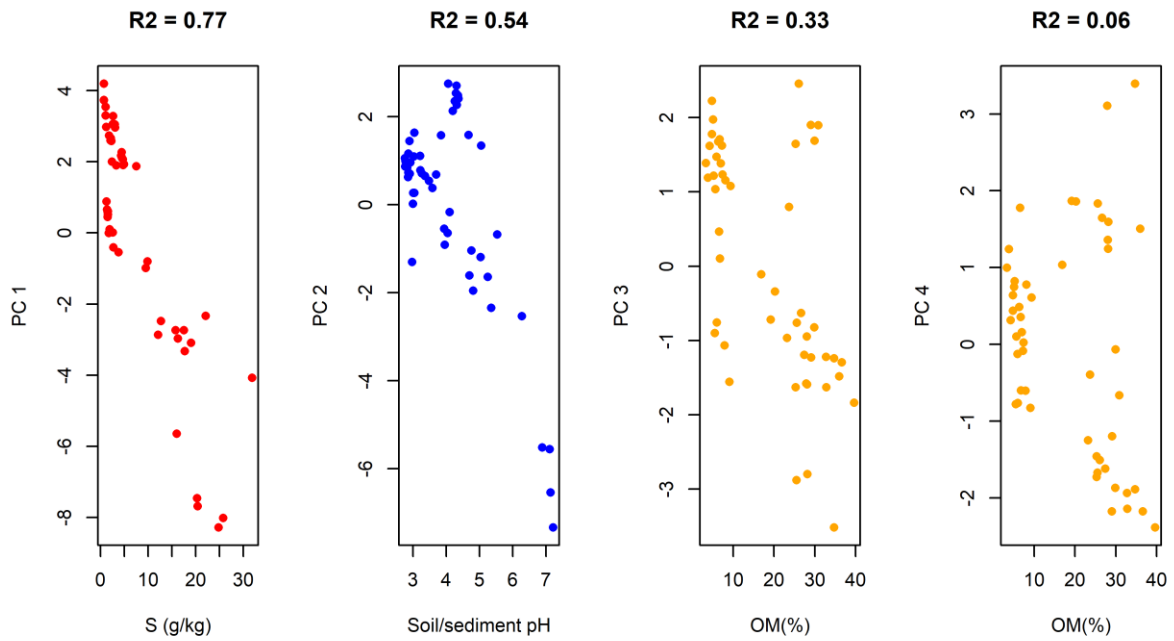


Fig. S9. Relationship between the first four principal components (PC1, PC2, PC3, PC4) and their potential explanatory variables, i.e., S concentration (in g/kg), soil and sediment pH, and soil organic matter (OM, in %). R^2 values indicate the proportion of variance explained by the soil properties: 0.77 for PC1 vs. S, 0.54 for PC vs. pH, 0.33 for PC3 vs. OM, and 0.06 for PC4 vs. OM.

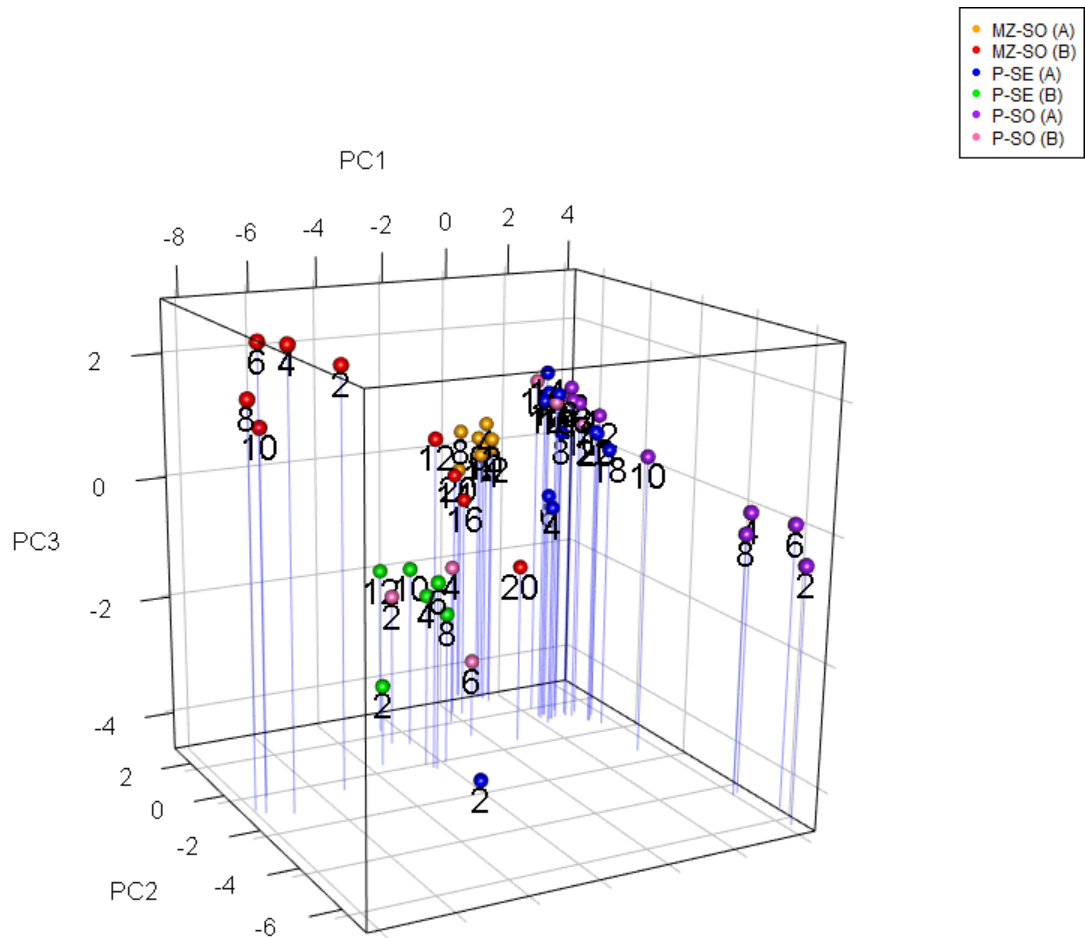


Fig. S10. Three-dimensional score plot based on the first three principal components (PC1, PC2, PC3) for depth profiles of soils and sediments from the precipitation pond (P) and mixing zone (MZ) of the Taraldrud site (locations in Fig. 1). Each data point represents a given core depth, with the numbering indicating cm from the surface. Different colors represent different cores (see figure legend).

Table S14. Concentration and calculated transfer factors (TF) of Th-232 and U-238 in vegetation collected at the reference site (R), precipitation pond (P) and mixing zone (MZ) of the Taraldrud site. Concentrations are given as average \pm 1 standard deviation of replicate samples (n = 3). No available data is indicated in the table as n.d. and thus for these species “soil-to-root” TF calculations were not applicable (n.a).

Species	Site	Th-232				U-238			
		Concentration		TF		Concentration		TF	
		Roots mg/kg	Shoots mg/kg	Soil-to-root	Soil-to-shoot	Roots mg/kg	Shoots mg/kg	Soil-to-root	Soil-to-shoot
Grass	R	0.85 \pm 0.02	0.0155 \pm 0.0004	6.94E-02	1.27E-03	413 \pm 14	1.94 \pm 0.09	1.21E+02	5.70E-01
	P	0.7 \pm 0.1	0.29 \pm 0.03	6.36E-02	2.48E-02	10.6 \pm 0.9	3.06 \pm 0.37	2.30E-01	6.65E-02
	MZ	1.2 \pm 0.1	0.041 \pm 0.003	5.69E-02	1.97E-03	325 \pm 29	0.04 \pm 0.01	3.24E-01	4.07E-05
Fern	R	0.81 \pm 0.02	0.035 \pm 0.002	6.65E-02	2.84E-03	1.7 \pm 0.1	0.04 \pm 0.02	4.91E-01	1.25E-02
	P	0.94 \pm 0.05	0.023 \pm 0.003	3.84E-02	9.46E-04	78.4 \pm 2.2	0.068 \pm 0.002	1.41E-01	1.23E-04
	MZ	1.1 \pm 0.1	0.032 \pm 0.002	5.40E-02	1.55E-03	4.1 \pm 0.1	0.10 \pm 0.03	3.84E-03	9.83E-05
Wood club-rush	P	3.61 \pm 0.05	0.22 \pm 0.01	1.47E-01	9.11E-03	153 \pm 2	7.84 \pm 0.17	2.76E-01	1.41E-02
Spruce (bud)	R	n.d.	0.013 \pm 0.001	n.a.	9.66E-04	n.d.	0.01 \pm 0.0001	n.a.	1.61E-03
	P	n.d.	0.0041 \pm 0.0005	n.a.	1.68E-04	n.d.	0.07 \pm 0.02	n.a.	1.24E-04
	MZ	n.d.	0.004 \pm 0.001	n.a.	2.00E-04	n.d.	0.053 \pm 0.002	n.a.	5.26E-05
Birch (leaf)	R	n.d.	0.017 \pm 0.003	n.a.	1.42E-03	n.d.	0.008 \pm 0.001	n.a.	2.22E-03
	P	n.d.	0.015 \pm 0.004	n.a.	6.16E-04	n.d.	0.04 \pm 0.01	n.a.	6.92E-05
	MZ	n.d.	0.010 \pm 0.002	n.a.	4.75E-04	n.d.	0.16 \pm 0.02	n.a.	1.61E-04
European alder (leaf)	R	n.d.	0.011 \pm 0.003	n.a.	9.39E-04	n.d.	0.01 \pm 0.01	n.a.	3.29E-03
	MZ	n.d.	0.007 \pm 0.001	n.a.	3.32E-04	n.d.	0.030 \pm 0.002	n.a.	2.94E-05

References

1. T. Vidmar, EFFTRAN—A Monte Carlo efficiency transfer code for gamma-ray spectrometry, *Nuclear Instruments and Methods in Physics Research Section A: Accelerators, Spectrometers, Detectors and Associated Equipment*, 2005, **550**, 603-608.
2. P. R. Willmott, D. Meister, S. J. Leake, M. Lange, A. Bergamaschi, M. Böge, M. Calvi, C. Cancellieri, N. Casati, A. Cervellino, Q. Chen, C. David, U. Flechsig, F. Gozzo, B. Henrich, S. Jäggi-Spielmann, B. Jakob, I. Kalichava, P. Karvinen, J. Krempasky, A. Lüdeke, R. Lüscher, S. Maag, C. Quitmann, M. L. Reinle-Schmitt, T. Schmidt, B. Schmitt, A. Streun, I. Vartiainen, M. Vitins, X. Wang and R. Wulschleger, The Materials Science beamline upgrade at the Swiss Light Source, *J Synchrotron Radiat*, 2013, **20**, 667-682.
3. NGI, *E6 Taraldrud Alunskifer tiltaksplan: Supplerende grunnundersøkelser*, 2021.
4. W. Dong and S. C. Brooks, Determination of the formation constants of ternary complexes of uranyl and carbonate with alkaline earth metals (Mg²⁺, Ca²⁺, Sr²⁺, and Ba²⁺) using anion exchange method, *Environ Sci Technol*, 2006, **40**, 4689-4695.
5. H. Ervanne, E. Puukko and M. Hakanen, *Modeling of Sorption of Eu, Mo, Nb, Ni, Pa, Se, Sn, Th and U on Kaolinite and Illite in Olkiluoto Groundwater Simulants - Working Report 2013-31*, Olkiluoto, 2013.
6. E. Giffaut, M. Grivé, P. Blanc, P. Vieillard, E. Colàs, H. Gailhanou, S. Gaboreau, N. Marty, B. Madé and L. Duro, Andra thermodynamic database for performance assessment: ThermoChimie, *Applied Geochemistry*, 2014, **49**, 225-236.
7. M. Eisenbud and T. Gesell. Chapter 6 - Natural Radioactivity. In: M. Eisenbud and T. Gesell, editors. *Environmental Radioactivity (Fourth Edition)*, DOI: <https://doi.org/10.1016/B978-012235154-9/50010-4>. San Diego: Academic Press; 1997. p. 134-200.
8. Norwegian Environmental Agency, Quality standards for water, sediment and biota (M-608). *Journal*, 2016.
9. EU, Directive 2013/39/EU of the European Parliament and of the Council. *Journal*, 2013.
10. Canadian Council of Ministers of the Environment, Water Quality Guidelines for the Protection of Aquatic Life., <https://ccme.ca/en/current-activities/canadian-environmental-quality-guidelines>, 2023).
11. P. A. Beck and R. Jaques, *Datarapport for miljøgifter i Norge*, Oslo, 1993.
12. Ympäristöministeriö, *Maaperän pilaantuneisuuden ja puhdistustarpeen arviointi - ympäristöhallinnon ohjeita 2*, Helsinki, 2007.
13. Canadian Council of Ministers of the Environment, Canadian Soil Quality Guidelines for the Protection of Environmental and Human Health - Uranium 2007. *Journal*, 2007.
14. NEA, *Veileder for risikovurdering av forurenset sediment; M-409 Guidelines for risk assessment of contaminated sediments*, 2015.